

Original article

A database of thermodynamic properties of the reactions of glycolysis, the tricarboxylic acid cycle, and the pentose phosphate pathway

Xin Li, Fan Wu, Feng Qi and Daniel A. Beard*

Department of Physiology, Medical College of Wisconsin, 8701 Watertown Plank Road, Milwaukee, WI 53226, USA

*Corresponding author: Tel: +1 414 955 5752; Fax: +1 414 955 6568; Email: beardda@gmail.com

Submitted 15 October 2010; Revised 28 February 2011; Accepted 1 March 2011

A database of thermodynamic properties is developed, which extends a previous database of glycolysis and tricarboxylic acid cycle by adding the reactions of the pentose phosphate pathway. The raw data and documented estimations of solution properties are made electronically available. The database is determined by estimation of a set of parameters representing species-level free energies of formation. The resulting calculations provide thermodynamic and network-based estimates of thermodynamic properties for six reactions of the pentose phosphate pathway for which estimates are not available in the preexisting literature. Optimized results are made available in ThermoML format. Because calculations depend on estimated hydrogen and metal cation dissociation constants, an uncertainty and sensitivity analysis is performed, revealing 23 critical dissociation constants to which the computed thermodynamic properties are particularly sensitive.

Database URL: <http://www.biocoda.org/thermo>

Introduction

Reliable and self-consistent databases of thermodynamic properties for biochemical reactions are necessary for accurate analysis of biochemical systems (1–6). A recently developed database of thermodynamic properties for the reactions of glycolysis and the tricarboxylic acid cycle that was constituted from measured equilibrium data (7) represents a refinement to the Alberty database (8) in that it accounts for the ionic strength and interactions of biochemical reactants and metal cations (Mg^{2+} , Ca^{2+} , Na^+ and K^+) in estimating the derived properties from the raw data. The database of Li *et al.* (7) is a framework that can be extended and refined by adding the underlying raw experimental data in the database and/or refining the underlying model assumptions. Here an updated database is developed by adding the reactions of the pentose phosphate pathway into the original database.

As in Li *et al.* (7), thermodynamic properties (reference $\Delta_r G^0$ and $\Delta_r H^0$) values are estimated by minimizing the difference between model predictions and experimental data. Apparent equilibrium constants for biochemical reactions are estimated by these derived thermodynamic properties and compared to experimental data measured under non-standard conditions. The basic formulae described in Li *et al.* (7) are used here, which account for temperature, ionic interactions and ion binding (8–13) effects to convert standard-state reference quantities to experimental state quantities.

Input data

Database of measured equilibrium constants

Raw experimental data are obtained from original reports (14–19). As in Li *et al.* (7), we preferentially select studies

rated as A- and B-quality by Goldberg *et al.* (20–22). Free cation concentrations and ionic strength associated with these original studies are estimated based on the conditions reported in the original sources. All data and calculations are explicitly documented in the database. As we have previously established (7), each measurement entry in the raw-data database provides the following information: (i) enzyme name (EC number); (ii) experimental temperature, pH, ionic strength, apparent equilibrium constant, free metal cation concentrations, buffer and experimental method; (iii) quality rating from Goldberg *et al.* (20–22); (iv) notes on experiments and strategies of estimations and approximations applied in calculations; and (v) reference information. Up-to-date versions of the experimental database are made available at the URL <http://www.biocoda.org/thermo>, or by contacting the authors.

Database of reactions and estimated standard reaction enthalpies

There are eight reactions in the pentose phosphate pathway: glucose 6-phosphate dehydrogenase (EC 1.1.1.49, G6PD), 6-phosphogluconolactonase (EC 3.1.1.31, PGL), 6-phosphogluconate dehydrogenase (EC 1.1.1.44, PGD), ribose-5-phosphate isomerase (EC 5.3.1.6, R5PI), ribulose-phosphate 3-epimerase (EC 5.1.3.1, RUPE), transketolase (EC 2.2.1.1, TKL), transaldolase (EC 2.2.1.2, TAL) and transketolase 2 (EC 2.2.1.1, TKL2). The first three reactions are the oxidative pentose phosphate pathway, and the rest are the reductive pentose phosphate pathway (23). After adding these reactions into our original database, there are 33 reactions in total, which are shown in the Table 1 (first 33 reactions). Table 1 lists EC numbers, reaction names and the abbreviations employed, the reference reaction stoichiometries, and estimated standard reaction enthalpies at $T=298.15\text{K}$, $I=0\text{M}$. In the reference reaction, a superscript is used to indicate the charge of chemical species. For example, the abbreviation for references species for glucose (GLC^0) is distinguished from the abbreviation for the biochemical reactant GLC.

Reaction enthalpies ($\Delta_r H^0$) for two reactions in the pentose phosphate pathway (PGD and R5PI) can be estimated using van't Hoff equation because data on apparent equilibrium constants at different temperatures are available. Neither equilibrium data at different temperatures nor prior values of $\Delta_r H^0$ are available for the other six reactions of the pentose phosphate pathway; hence the symbol '#' is used to denote the absence of data. For these cases, the value is set to zero in further calculations.

Database of reactant and dissociation constants

There are seven reactants introduced to the reactant database by adding the pentose phosphate pathway into the thermodynamic database: erythrose 4-phosphate (E4P),

6-phosphoglucono- δ -lactone (PGLT), 6-phospho-D-gluconate (PGN), ribose 5-phosphate (R5P), ribulose 5-phosphate (RU5P), sedoheptulose 7-phosphate (S7P) and xylulose 5-phosphate (X5P). For the five sugar phosphates (E4P, R5P, RU5P, S7P and X5P), cation dissociation constants for only R5P can be found in NIST database. Since E4P, RU5P, S7P and X5P are structurally similar substances to R5P (all have similar near neighbors to the phosphate group), a pragmatic approach to estimate the necessary dissociation constants is to use the values for R5P (24). Specifically, E4P, RU5P, S7P and X5P are assumed to have dissociation properties equal to those for R5P in our calculations. For PGLT, we use the pK_{H1} value of 5.99 from Alberty (10). For PGN, Casazza *et al.* (15) report that the hydrogen ion dissociation constant for the carboxylic acid is $>1.0E-4$, while the constant for the phosphate ester is the same as that of glucose 6-P [$pK_{H1}=5.99$ (10)]. Here we arbitrarily assign the value of 4.995 to the pK_{H1} for PGN, which is the average of 4 and 5.99. The uncertainties of these assignments are considered in the uncertainty and sensitivity analysis below.

Basic thermodynamic and ion binding data for biochemical reactants and associated reference species are listed in Table 2. Each entry in the table contains the following information: (i) detailed name of reactant; (ii) reference species abbreviation; (iii) reactant abbreviation; (iv) number of protons in reference species; and (v) the dissociation constants (provided as pK) and the corresponding dissociation enthalpies $\Delta_d H_{K_d}$. Dissociation constants and enthalpies are tabulated at 298.15 K and 0.1 M ionic strength. The symbol '#' is used to indicate absence of data. For these cases, the pK 's are assumed to be infinite (no binding) with corresponding dissociation constants equal to zero. In the calculations, all the pK and $\Delta_d H_{K_d}$ values are adjusted to a common reference state of $T=298.15\text{K}$ and $I=0$.

Estimation of standard-state thermodynamic quantities

Given the compiled raw experimental data on the reactions and reactants, the thermodynamic model is used to estimate reference $\Delta_r G^0$ and $\Delta_f G_f^0$ values for the reference reactions and species. Note that in our thermodynamic model the $\Delta_f G_f^0$ values are adjustable parameters estimated to obtain the best fit to the biochemical equilibrium data. As in previous studies (8), values of $\Delta_f G_f^0$ for oxidized species of certain redox pairs are arbitrarily set to zero. Thus, these values are not true free energies of the reactions of formation for these chemical species; instead, they are parameters for which the thermodynamic model makes optimal predictions for these interdependent biochemical reactions.

Table 1. Reactions with standard reaction enthalpies $\Delta_r H^0$ estimated for $I=0$

EC No.	Reaction name	Reaction abbreviation	Reference reaction	$\Delta_r H^0$ (kJ/mol)
EC 2.7.1.1	Glucokinase	GLK	$\text{GLC}^0 + \text{ATP}^{4-} = \text{G6P}^{2-} + \text{ADP}^{3-} + \text{H}^+$	-23.8 ^a
EC 5.3.1.9	Phosphoglucose isomerase	PGI	$\text{G6P}^{2-} = \text{F6P}^{2-}$	11.53 ^b
EC 2.7.1.11	Phosphofruktokinase	PFK	$\text{F6P}^{2-} + \text{ATP}^{4-} = \text{F16P}^{4-} + \text{ADP}^{3-} + \text{H}^+$	-9.5 ^c
EC 4.1.2.13	Fructose-1,6-bisphosphatase aldolase	FBA	$\text{F16P}^{4-} = \text{DHAP}^{2-} + \text{GAP}^{2-}$	48.97 ^b
EC 5.3.1.1	Triosphosphate isomerase	TPI	$\text{GAP}^{2-} = \text{DHAP}^{2-}$	2.73 ^d
EC 4.1.2.13	Fructose-1,6-bisphosphatase aldolase 2	FBA2	$\text{F16P}^{4-} = 2\text{DHAP}^{2-}$	51.70 ^b
EC 1.2.1.12	Glyceraldehyde-3-P dehydrogenase	GAP	$\text{GAP}^{2-} + \text{HPO}_4^{2-} + \text{NAD}_{\text{ox}}^- = \text{BPG}^{4-} + \text{NAD}_{\text{red}}^{2-} + \text{H}^+$	# ^e
EC 2.7.2.3	Phosphoglycerate kinase	PGK	$\text{GAP}^{2-} + \text{HPO}_4^{2-} + \text{NAD}_{\text{ox}}^- + \text{ADP}^{3-} = \text{PG3}^{3-} + \text{NAD}_{\text{red}}^{2-} + \text{ATP}^{4-} + \text{H}^+$	# ^e
EC 5.4.2.1	Phosphoglycerate mutase	PGYM	$\text{PG2}^{3-} = \text{PG3}^{3-}$	28.05 ^b
EC 4.2.1.11	Enolase	ENO	$\text{PG2}^{3-} = \text{PEP}^{3-} + \text{H}_2\text{O}^0$	15.1 ^b
EC 2.7.1.40	Pyruvate kinase	PYK	$\text{PYR}^- + \text{ATP}^{4-} = \text{PEP}^{3-} + \text{ADP}^{3-} + \text{H}^+$	5.415 ^a
EC 4.1.3.7	Citrate synthase	CITS	$\text{OAA}^{2-} + \text{AcCoA}^0 + \text{H}_2\text{O}^0 = \text{CIT}^{3-} + \text{CoAS}^- + 2\text{H}^+$	# ^e
EC 4.2.1.3	Aconitrate hydratase	ACON	$\text{ISCIT}^{3-} = \text{CIT}^{3-}$	-20.0 ^b
EC 1.1.1.42	Isocitrate dehydrogenase	IDH	$\text{ISCIT}^{3-} + \text{NADP}_{\text{ox}}^{3-} + \text{H}_2\text{O}^0 = \text{AKG}^{2-} + \text{NADP}_{\text{red}}^{4-} + \text{CO}_3^{2-} + 2\text{H}^+$	-22.17 ^b
EC 6.2.1.4	Auccinate-CoA ligase	SCS	$\text{GTP}^{4-} + \text{SUC}^{2-} + \text{CoAS}^- + \text{H}^+ = \text{GDP}^{3-} + \text{HPO}_4^{2-} + \text{SUCCoA}^-$	-30.9 ^b
EC 4.2.1.2	Fumarate hydratase	FUM	$\text{FUM}^{2-} + \text{H}_2\text{O}^0 = \text{MAL}^{2-}$	-13.18 ^b
EC 1.1.1.37	Malate dehydrogenase	MDH	$\text{MAL}^{2-} + \text{NAD}_{\text{ox}}^- = \text{OAA}^{2-} + \text{NAD}_{\text{red}}^{2-} + \text{H}^+$	51.29 ^b
EC 2.7.4.6	Nucleoside-diphosphate kinase	NDK	$\text{ATP}^{4-} + \text{GDP}^{3-} = \text{ADP}^{3-} + \text{GTP}^{4-}$	# ^e
EC 1.6.1.1	NADP transhydrogenase	NPTH	$\text{NAD}_{\text{ox}}^- + \text{NADP}_{\text{red}}^{4-} = \text{NAD}_{\text{red}}^{2-} + \text{NADP}_{\text{ox}}^{3-}$	-4.1 ^c
EC 1.1.1.40	Malic enzyme	MLE	$\text{MAL}^{2-} + \text{NADP}_{\text{ox}}^{3-} + \text{H}_2\text{O}^0 = \text{PYR}^- + \text{NADP}_{\text{red}}^{4-} + \text{CO}_3^{2-} + 2\text{H}^+$	# ^e
EC 1.1.1.37	Malate dehydrogenase 2	MDH2	$\text{MAL}^{2-} + \text{AcCoA}^0 + \text{NAD}_{\text{ox}}^- + \text{H}_2\text{O}^0 = \text{CIT}^{3-} + \text{CoAS}^- + \text{NAD}_{\text{red}}^{2-} + 3\text{H}^+$	# ^e
EC 2.7.1.23	NAD ⁺ kinase	NADK	$\text{ATP}^{4-} + \text{NAD}_{\text{ox}}^- = \text{ADP}^{3-} + \text{NADP}_{\text{ox}}^{3-} + \text{H}^+$	# ^e
EC 3.6.1.32	ATPase	ATPS	$\text{ATP}^{4-} + \text{H}_2\text{O}^0 = \text{ADP}^{3-} + \text{HPO}_4^{2-} + \text{H}^+$	-20.5 ^a
EC 3.1.3.1	Alkaline phosphatase/G6P hydrolysis	G6PH	$\text{G6P}^{2-} + \text{H}_2\text{O}^0 = \text{GLC}^0 + \text{Pi}^{2-}$	0.91 ^a
EC 6.4.1.1	Pyruvate carboxylase	PCL	$\text{PYR}^- + \text{ATP}^{4-} + \text{CO}_3^{2-} = \text{OAA}^{2-} + \text{ADP}^{3-} + \text{Pi}^{2-}$	# ^e
EC 1.1.1.49	Glucose 6-phosphate dehydrogenase	G6PD	$\text{G6P}^{2-} + \text{NADP}_{\text{ox}}^{3-} = \text{PGLT}^{2-} + \text{NADP}_{\text{red}}^{4-} + \text{H}^+$	# ^e
EC 3.1.1.31	6-Phosphogluconolactonase	PGL	$\text{G6P}^{2-} + \text{NADP}_{\text{ox}}^{3-} + \text{H}_2\text{O}^0 = \text{PGN}^{3-} + \text{NADP}_{\text{red}}^{4-} + 2\text{H}^+$	# ^e
EC 1.1.1.44	6-Phosphogluconate dehydrogenase	PGD	$\text{PGN}^{3-} + \text{NADP}_{\text{ox}}^{3-} + \text{H}_2\text{O}^0 = \text{RU5P}^{2-} + \text{NADP}_{\text{red}}^{4-} + \text{CO}_3^{2-} + 2\text{H}^+$	37.47 ^b
EC 5.3.1.6	Ribose-5-phosphate isomerase	R5PI	$\text{R5P}^{2-} = \text{RU5P}^{2-}$	12.86 ^b
EC 5.1.3.1	Ribulose-phosphate 3-epimerase	RUPE	$\text{RU5P}^{2-} = \text{X5P}^{2-}$	# ^e
EC 2.2.1.1	Transketolase	TKL	$\text{S7P}^{2-} + \text{GAP}^{2-} = \text{R5P}^{2-} + \text{X5P}^{2-}$	# ^e
EC 2.2.1.2	Transaldolase	TAL	$\text{S7P}^{2-} + \text{GAP}^{2-} = \text{E4P}^{2-} + \text{F6P}^{2-}$	# ^e
EC 2.2.1.1	Transketolase 2	TKL2	$\text{F6P}^{2-} + \text{GAP}^{2-} = \text{E4P}^{2-} + \text{X5P}^{2-}$	# ^e
EC 1.2.4.1+EC 2.3.1.12+EC 1.8.1.4	Pyruvate dehydrogenase complex	PDH	$\text{PYR}^- + \text{CoAS}^- + \text{NAD}_{\text{ox}}^- + \text{H}_2\text{O} = \text{CO}_3^{2-} + \text{AcCoA}^0 + \text{NAD}_{\text{red}}^{2-} + \text{H}^+$	# ^e
EC 1.1.1.41	Isocitrate dehydrogenase	IDH2	$\text{ISCIT}^{3-} + \text{NAD}_{\text{ox}}^- + \text{H}_2\text{O}^0 = \text{AKG}^{2-} + \text{NAD}_{\text{red}}^{2-} + \text{CO}_3^{2-} + 2\text{H}^+$	-26.27 ^d
EC 1.2.1.52	α -Ketoglutarate dehydrogenase	AKGDH	$\text{AKG}^{2-} + \text{NAD}_{\text{ox}}^- + \text{CoAS}^- + \text{H}_2\text{O}^0 = \text{SUCCoA}^- + \text{NAD}_{\text{red}}^{2-} + \text{CO}_3^{2-} + \text{H}^+$	# ^e
EC 1.3.5.1	Succinate dehydrogenase	SDH	$\text{SUC}^{2-} + \text{CoQ}^0 = \text{FUM}^{2-} + \text{CoQH}_2^0$	# ^e

^aGoldberg *et al.* (21, 33).^bCalculated value based on experimental data at different temperatures.^cValues obtained from Goldberg *et al.* (20, 21) where associated ionic strength is not reported.^dValue calculated from sum of dependent reactions.^eValue not available.

Table 2. Reactant database^a

Reactant	Reference species abbreviation ^b	Reactant abbreviation	N_H^b	pK_{H1}	$\Delta_d H_{H1}$	pK_{H2}	$\Delta_d H_{H2}$	pK_{Mg1}	$\Delta_d H_{Mg1}$	pK_{HMg}	$\Delta_d H_{HMg}$	pK_{Mg2}	$\Delta_d H_{Mg2}$	pK_{K1}	$\Delta_d H_{K1}$	pK_{Na1}	$\Delta_d H_{Na1}$	pK_{HNa}	$\Delta_d H_{HNa}$	pK_{Ca1}	$\Delta_d H_{Ca1}$	pK_{HCa}	$\Delta_d H_{HCa}$
Acetyl-coenzyme A	ACoA ⁰	ACoA	3	#	#	#	#	#	#	#	#	#	#	#	#	#	#	#	#	#	#	#	#
Adenosine diphosphate	ADP ³⁻	ADP	12	6.496	-2	3.87	16	3.3	-15	1.59	-7.5	1.27	-11.76	1	#	1.12	#	#	#	2.86	-9.6	1.48	-6.2
Adenosine triphosphate	ATP ⁴⁻	ATP	12	6.71	-2	3.99	15	4.28	-18	2.32	-9.6	1.7	-17.52	1.17	-1	1.31	0.8	#	#	3.95	-13	2.16	-7.9
1,3-Bisphosphoglycerate	BPG ⁴⁻	BPG	4	7.1 ^c	#	#	#	#	#	#	#	#	#	#	#	#	#	#	#	#	#	#	#
Citrate	CIT ³⁻	CIT	5	5.67	-1.9	4.35	3.1	3.517	-8	1.8	#	#	#	0.6	-3.54	0.75	-1	#	#	3.54	-1.2	2.07	#
Coenzyme A-SH	COAS ⁻	COAS	0	8.17 ^c	#	#	#	#	#	#	#	#	#	#	#	#	#	#	#	#	#	#	#
Carbon dioxide (total)	CO ₂ ²⁻	CO ₂ _tot	0	9.9 ^c	16.1 ^c	6.15 ^c	8.27 ^c	#	#	#	#	#	#	#	#	#	#	#	#	#	#	#	#
Dihydroxyacetone phosphate	DHAP ²⁻	DHAP	5	5.9	#	#	#	1.57	#	#	#	#	#	#	#	#	#	#	#	#	#	#	#
D-fructose 6-phosphate	F6P ²⁻	F6P	11	5.89	-0.559 ^d	1.1	#	1.74 ^e	-9.72 ^d	#	#	#	#	#	#	#	#	#	#	1.38	#	#	#
D-fructose 1,6-phosphate	F16P ⁴⁻	F16P	10	6.64	#	5.92	#	2.7	#	2.12	#	#	#	#	#	#	#	#	#	#	#	#	#
Fumarate	FUM ²⁻	FUM	2	4.09	-1.56	2.86	1.08	#	#	#	#	#	#	#	#	#	#	#	#	0.6	-6.44	#	#
D-glucose 6-phosphate	G6P ²⁻	G6P	11	5.89 ^e	-0.559 ^d	#	#	1.74 ^b	-9.72 ^d	#	#	#	#	#	#	#	#	#	#	#	#	#	#
D-glyceraldehyde 3-phosphate	GAP ²⁻	GAP	5	5.27 ^c	#	#	#	#	#	#	#	#	#	#	#	#	#	#	#	#	#	#	#
Guanosine diphosphate	GDP ³⁻	GDP	12	6.505	-2.14	2.8	#	3.4	-7.1	#	#	#	#	#	#	#	#	#	#	#	#	#	#
D-glucose	GLC ⁰	GLC	12	#	#	#	#	#	#	#	#	#	#	#	#	#	#	#	#	#	#	#	#
Guanosine triphosphate	GTP ⁴⁻	GTP	12	6.63	-3	2.93	7.1	4.31	-17	2.31	#	#	#	#	#	#	#	#	#	3.7	#	#	#
Water	H ₂ O ⁰	H ₂ O	2	#	#	#	#	#	#	#	#	#	#	#	#	#	#	#	#	#	#	#	#
Isocitrate	ISCI ³⁻	ISCI	5	5.765	#	4.29	#	2.625	#	1.43	#	#	#	#	#	#	#	#	#	2.54	#	#	#
α -Ketoglutarate	AKG ²⁻	AKG	4	#	#	#	#	#	#	#	#	#	#	#	#	#	#	#	#	#	#	#	#
Malate	MAL ²⁻	MAL	4	4.715	-0.58	3.265	3.4	1.71	-6.16	0.9 ^f	#	#	#	0.18	-2.86	0.28	0.4	#	#	2.005	-1.06	1.06	8
NAD _{ox}	NAD _{ox} ⁻	NAD _{ox}	26	#	#	#	#	#	#	#	#	#	#	#	#	#	#	#	#	#	#	#	#
NAD _{red}	NAD _{red} ²⁻	NAD _{red}	27	#	#	#	#	#	#	#	#	#	#	#	#	#	#	#	#	#	#	#	#
NADP _{ox}	NADP _{ox} ³⁻	NADP _{ox}	25	6.255 ^k	#	3.874 ^k	#	#	#	#	#	#	#	#	#	#	#	#	#	#	#	#	#
NADP _{red}	NADP _{red} ⁴⁻	NADP _{red}	26	6.255 ^l	#	3.874 ^l	#	#	#	#	#	#	#	#	#	#	#	#	#	#	#	#	#

(Continued)

Table 2. Continued.

Reactant	Reference species abbreviation ^b	Reactant abbreviation	N_i^b	pK_{i1}	$\Delta_d H_{i1}$	pK_{i2}	$\Delta_d H_{i2}$	pK_{iMg}	$\Delta_d H_{iMg}$	pK_{iMg2}	$\Delta_d H_{iMg2}$	pK_{iMg1}	$\Delta_d H_{iMg1}$	pK_{iMg3}	$\Delta_d H_{iMg3}$	pK_{Ca1}	$\Delta_d H_{Ca1}$	pK_{H1Ca}	$\Delta_d H_{H1Ca}$		
Oxaloacetate	OAA ²⁻	OAA	2	3.9	5.24	2.26	16.62	1.02	#	#	#	#	#	#	#	1.6	#	#	#		
Orthophosphate	HPO ₄ ²⁻	Pi	1	6.78	4.6	1.945	-8.7	1.823	-9.518	0.669	#	#	#	0.0856	#	1.745	-9.518	0.921	-10.759		
2-Phospho-D-glycerate	PG2 ³⁻	PG2	4	7	#	3.55	#	2.45	#	#	#	#	#	#	#	#	#	#	#		
3-Phospho-D-glycerate	PG3 ³⁻	PG3	4	6.89 ^c	#	3.64 ^g	#	2.21 ^h	#	#	#	#	#	#	#	0.87 ^h	#	#	#		
Phosphoenolpyruvate	PEP ²⁻	PEP	2	6.245	#	3.45	#	2.26	#	#	#	#	#	#	#	1.08	#	#	#		
Pyruvate	PYR ⁻	PYR	3	2.26	12.8	#	#	1.1	#	#	#	#	#	#	#	#	#	#	#		
Succinate	SUC ²⁻	SUC	4	5.275	0.41	4.02	3	1.355	#	0.62	#	#	0.43	-2.76	0.4212	-2.759	#	1.405	-8.939	0.65	-8
Succinyl-CoA	SUCCoA ⁻	SUCCoA	4	3.99 ^c	#	#	#	#	#	#	#	#	#	#	#	#	#	#	#	#	
Erythrose 4-phosphate	E4P ²⁻	E4P	9	6.255 ⁱ	-9.75 ⁱ	2 ⁱ	#	1.58 ⁱ	-9.71 ⁱ	#	#	#	#	#	#	1.48 ⁱ	#	#	#	#	
6-Phosphoglucono-δ-lactone	PGLT ²⁻	PGLT	11	5.99 ^c	#	#	#	#	#	#	#	#	#	#	#	#	#	#	#	#	
6-Phosphogluconate	PGN ³⁻	PGN	13	4.995 ^j	#	#	#	#	#	#	#	#	#	#	#	#	#	#	#	#	
Ribose 5-phosphate	R5P ²⁻	R5P	11	6.255	-9.75	2	#	1.58	-9.71 ^d	#	#	#	#	#	#	1.48	#	#	#	#	
Ribulose 5-phosphate	RU5P ²⁻	RU5P	11	6.255 ⁱ	-9.75 ⁱ	2 ⁱ	#	1.58 ⁱ	-9.71 ⁱ	#	#	#	#	#	#	1.48 ⁱ	#	#	#	#	
Sedoheptulose 7-phosphate	S7P ²⁻	S7P	15	6.255 ⁱ	-9.75 ⁱ	2 ⁱ	#	1.58 ⁱ	-9.71 ⁱ	#	#	#	#	#	#	1.48 ⁱ	#	#	#	#	
Xylulose 5-phosphate	X5P ²⁻	X5P	11	6.255 ⁱ	-9.75 ⁱ	2 ⁱ	#	1.58 ⁱ	-9.71 ⁱ	#	#	#	#	#	#	1.48 ⁱ	#	#	#	#	

^aDissociation pK and $\Delta_d H_{iKd}$ are reported for $T=298.15\text{ K}$ and $I=0.1\text{ M}$. Unless indicated, values are the average number obtained from NIST database (27). Dissociation enthalpies are reported in units of kJ/mol . Subscripts on ' pK ' and ' $\Delta_d H$ ' entries are defined as follows: 'H': hydrogen, 'Mg': magnesium, 'K': potassium, 'Na': sodium, 'Ca': calcium, '1': first ion dissociation, '2': second ion dissociation, 'HMg': hydrogen ion binds to the ligand before magnesium ion binds to the ligand. '#' denotes value is not available.

^bAlberty (8).

^cAlberty (10, 34).

^dTewari *et al.* (35).

^eG6P and F6P are assumed to have equivalent H⁺ and Mg²⁺-dissociation properties.

^fFrom NIST database (36) at $T=293.15\text{ K}$.

^gLarsson-Raźnikiewicz (37).

^hMerrill *et al.* (38).

ⁱCasazza *et al.* (15).

^kBriggs *et al.* (39).

^lNADP_{red} is assumed to have equivalent dissociation properties as NADP_{ox}.

^jE4P, RU5P, S7P and X5P are assumed to have equivalent dissociation properties as R5P (24).

Table 3. Values of $\Delta_f G_i^0$ ($T=298.15$ K, $l=0$) used in this study and that were taken from Alberty (8) (Table 3.2)

Species	$\Delta_f G_i^0$ (kJ/mol)
ACoA ⁰	-188.52
ADP ³⁻	-1906.13
CO ₃ ²⁻	-527.81
GTP ⁴⁻	-2768.1
H ₂ O	-237.19
NAD _{ox} ⁻	0 ^a
HPO ₄ ²⁻	-1096.1
H ⁺	0
CoQ ⁰	0 ^a
CoQH ₂ ⁰	-89.92

^aProperty value is based on the arbitrary assignment of zero.

Because the calculated $\Delta_f G_i^0$ are interrelated [e.g. in the reductive pentose phosphate pathway, five carbon sugars (X5P and R5P) are converted into three carbon (GAP) and six carbon (F6P) sugars which can then be utilized by the pathway of glycolysis], the database of $\Delta_f G_i^0$ may be rigorously extended only by recalculating the entire database using all of the raw data. Therefore, model fitting is based on total 686 data entries for the network of all 33 reactions (the first 33 reactions listed in Table 1). Standard free energies of formation for all the reference species are unable to be estimated independently because there are 29 stoichiometrically independent reactions and in total 40 reactants in our system. There are four reactions PDH, IDH2, AKGDH and SDH (last four reactions in Tables 1 and 4) in the TCA cycle for which direct measurements are not available in the literature. For these reactions, $\Delta_r G^0$ values are calculated using Alberty's database (8) and set as constraints to perform the optimization of the thermodynamic model. IDH2 is not an independent reaction in the overall network of 33 reactions. Therefore, values of $\Delta_f G_i^0$ for 32 reference species may be estimated from data on the 29 reactions with the three constraints. The values of $\Delta_f G_i^0$ for eight species are set to fixed values which are obtained from Alberty (8), as shown in Table 3 (values of $\Delta_f G_i^0$ for CoQ⁰ and CoQH₂⁰ do not come into these calculations). A constrained nonlinear optimization procedure with the *fmincon* solver (Mathworks, Inc.) is used to analyze the whole data set. By weighting in inverse proportion to the number of data points available for a given reaction and minimizing the difference between model predictions and experimental data, a simultaneous solution of standard reaction Gibbs energies is obtained for the entire data set.

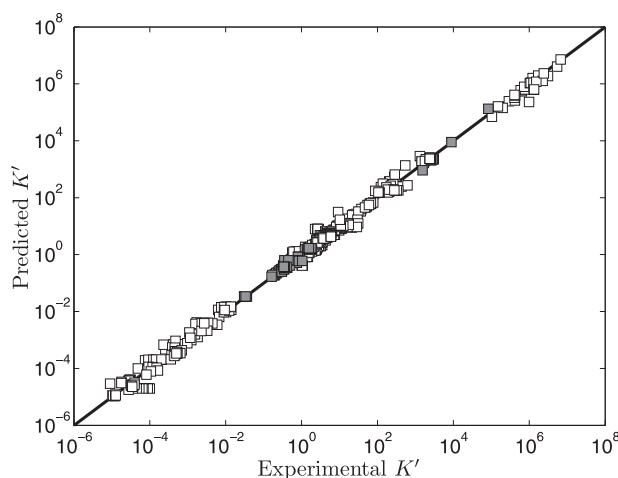


Figure 1. Model-predicted K' versus experimental K' . Model predicted apparent equilibrium constants under defined experimental conditions (T , l , $[Mg^{2+}]$, $[Ca^{2+}]$, $[Na^+]$, $[K^+]$ and pH) are plotted versus experimental measurements for all data used in the analysis. Data points in the pentose phosphate pathway are shown as filled squares.

Results

Estimated Gibbs free energies of reaction and formation

Figure 1 illustrates model predictions versus experimental data for all data used in the analysis. The predicted K' values are obtained based on accounting for the biochemical state associated with a given experimental measurement in the raw-data database. Data points in the pentose phosphate pathway are shown as filled squares. Other data points are shown as open squares. The data span almost 14 orders of magnitude, and reveal good agreement between model predictions and measured data.

The optimal estimates of $\Delta_r G^0$ listed in Table 4 ($\Delta_r G_n^0$), compared to the values from Li *et al.* (7) ($\Delta_r G_o^0$). $\Delta_r G^0$ of first 25 reactions are almost the same as the results obtained previously (7). For the remaining eight reactions of the pentose phosphate pathway, since the $\Delta_f G_i^0$ of the reference species for E4P, PGLT, PGN and S7P are not available in the Alberty (8) or Goldberg's database (25), the symbol '#' is used to denote the lack of a value. For reactions R5PI and RUPE, the absolute difference between our current model predictions and the values reported by Goldberg *et al.* (25) is within a reasonable margin, 0.21 and 0.07 kJ/mol, respectively. Predicted K' versus experimental measures are plotted in Figure 2 for these two reactions (R5PI and RUPE). The current database and the Goldberg database yield similar results. Recall that the dissociation properties of R5P, RU5P and X5P are assumed to be the same; the binding polynomials for the reactants on the left- and right-hand sides of these reactions are identical.

Table 4. Optimal reaction free energies for reference chemical reactions ($\Delta_r G^0$) and for biochemical reactions ($\Delta_r G^0$) under physiological conditions^a

EC No.	Reaction	$\Delta_r G_n^0$ ^b	$\Delta_r G_o^0$ ^b	$\Delta_r G^0$	$\Delta_r G^0 - \Delta_r G_n^0$	Non-standard element contributions ^c			
						<i>T</i>	<i>I</i>	pH	<i>P</i>
EC 2.7.1.1	GLK	16.19	16.03	-19.22	-35.41	1.61	1.57	-41.56	2.97
EC 5.3.1.9	PGI	3.12	3.13	2.78	-0.34	-0.34	0	0	0
EC 2.7.1.11	PFK	26.79	26.79	-15.62	-42.41	1.46	-4.70	-41.56	2.40
EC 4.1.2.13	FBA	18.79	18.80	24.64	5.85	-1.21	6.26	0	0.81
EC 5.3.1.1	TPI	-7.01	-7.01	-7.57	-0.56	-0.39	0	0	-0.17
EC 4.1.2.13	FBA2	11.79	11.79	17.07	5.28	-1.61	6.26	0	0.64
EC 1.2.1.12	GAP	51.37	51.37	2.60	-48.77	2.07	-9.39	-41.56	0.12
EC 2.7.2.3	PGK	34.37	34.37	-19.00	-53.37	1.38	-9.39	-41.56	-3.79
EC 5.4.2.1	PGYM	-5.89	-5.90	-6.35	-0.46	-1.37	0	0	0.91
EC 4.2.1.11	ENO	-4.54	-4.53	-4.47	0.07	-0.79	0	0	0.86
EC 2.7.1.40	PYK	66.91	66.90	27.18	-39.73	2.48	-1.57	-41.56	0.92
EC 4.1.3.7	CITS	60.16	60.32	-36.60	-96.76	2.42	-6.26	-83.13	-9.80
EC 4.2.1.3	ACON	-5.75	-5.76	-7.58	-1.83	0.57	0	0	-2.41
EC 1.1.1.42	IDH	97.05	97.06	-3.29	-100.34	4.80	-6.26	-83.13	-15.76
EC 6.2.1.4	SCS	-56.55	-56.56	0.07	56.62	-1.03	6.26	41.56	9.82
EC 4.2.1.2	FUM	-3.38	-3.38	-3.52	-0.14	0.39	0	0	-0.53
EC 1.1.1.37	MDH	71.41	71.09	28.04	-43.37	0.81	-3.13	-41.56	0.52
EC 2.7.4.6	NDK	0.02	0.01	-0.56	-0.58	0	0	0	-0.58
EC 1.6.1.1	NPTH	-3.53	-3.58	-0.41	3.12	0.02	3.13	0	-0.03
EC 1.1.1.40	MLE	104.53	103.45	2.00	-102.53	4.21	-7.83	-83.13	-15.78
EC 1.1.1.37	MDH2	131.57	131.41	-6.50	-138.07	5.30	-9.39	-124.69	-9.28
EC 2.7.1.23	NADK	29.11	26.90	-9.95	-39.06	1.17	-1.57	-41.56	2.89
EC 3.6.1.32	ATPS	4.99	4.67	-32.42	-37.41	1.03	1.57	-41.56	1.56
EC 3.1.3.1	G6PH	-11.20	-11.36	-13.10	-1.90	-0.49	0	0	-1.41
EC 6.4.1.1	PCL	-24.60	-24.12	-4.57	20.03	-0.99	3.13	0	17.89
EC 1.1.1.49	G6PD	38.69	# ^d	-7.51	-46.20	1.56	-6.26	-41.56	0.07
EC 3.1.1.31	PGL	69.16	# ^d	-21.89	-91.05	2.78	-10.96	-83.13	0.25
EC 1.1.1.44	PGD	104.64	# ^d	1.23	-103.41	2.70	-6.26	-83.13	-16.73
EC 5.3.1.6	R5PI	0.99	1.2 ^e	0.52	-0.47	-0.47	0	0	0
EC 5.1.3.1	RUPE	-1.28	-1.21 ^e	-1.33	-0.05	-0.05	0	0	0
EC 2.2.1.1	TKL	1.58	# ^d	1.23	-0.35	0.06	0	0	-0.41
EC 2.2.1.2	TAL	2.72	# ^d	2.63	-0.09	0.11	0	0	-0.20
EC 2.2.1.1	TKL2	8.98	# ^d	8.71	-0.27	0.36	0	0	-0.63
EC 1.2.4.1+EC 2.3.1.12+EC 1.8.1.4	PDH	15.78 ^f	17.50	-39.26	-55.04	0.64	-4.70	-41.56	-9.43
EC 1.1.1.41	IDH2	93.52	93.48	-3.70	-97.22	4.82	-3.13	-83.13	-15.79
EC 1.2.1.52	AKGDH	15.85 ^f	15.28	-37.66	-53.51	0.64	-3.13	-41.56	-9.45
EC 1.3.5.1	SDH	-1.35 ^f	-3.10	-0.59	0.76	-0.05	0	0	0.81

^aThe physiological conditions (26) are as follows: $T=310.15\text{ K}$, $I=0.18\text{ M}$, $\text{pH}=7$, $[\text{Mg}^{2+}]=0.8\text{ mM}$, $[\text{K}^+]=140\text{ mM}$, $[\text{Na}^+]=10\text{ mM}$, $[\text{Ca}^{2+}]=0.0001\text{ mM}$. The unit of the free energy is kJ/mol.

^b $\Delta_r G_n^0$ is the optimal reaction free energies for reference chemical reactions in this work, $\Delta_r G_o^0$ is the optimal reaction free energies for reference chemical reaction in Li *et al.* (7).

^cThis column lists the actual values of each non-standard physiological condition contribution (in kJ/mol) to the difference between the physiological free energies ($\Delta_r G^0$) and the standard free energies ($\Delta_r G_n^0$). *T* denotes the temperature contribution, *I* denotes the ionic strength contribution, pH denotes the pH contribution and *P* denotes the binding polynomial contribution.

^dValue is not available.

^eCalculated from Goldberg's database (25): the $\Delta_r G_i^0$ values for R5P, RU5P and X5P in Goldberg's database are -1582.57, -1581.37 and -1582.58 kJ/mol, respectively.

^fValues calculated from Alberty's database (8) are used as model constraints for which there are no equilibrium data in the raw-data database. Since the $\Delta_r G_i^0$ values for CoQ and CoQH2 are not predicted here, these values are set to 0 and -89.92 kJ/mol, respectively [from Alberty (8)] to computed $\Delta_r G^0$ for the SDH reaction.

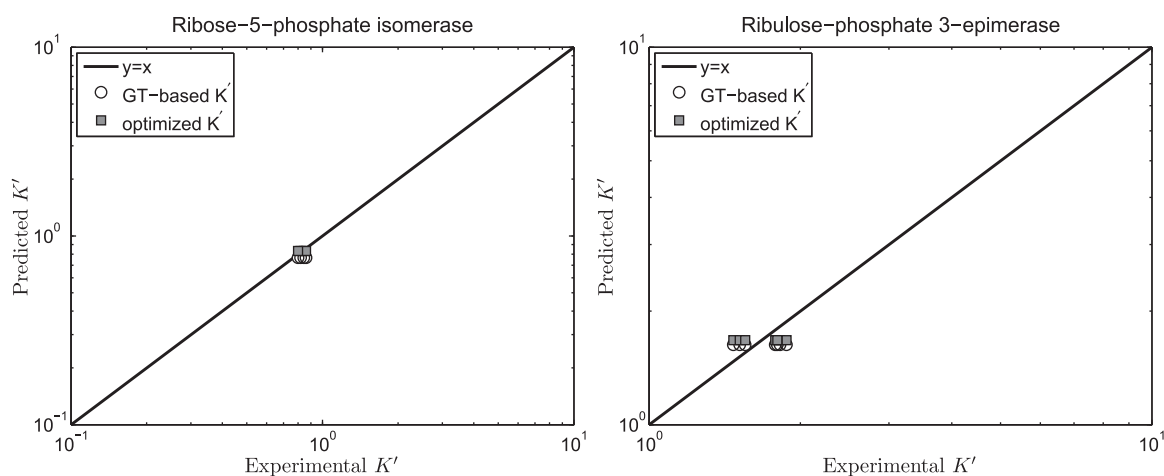


Figure 2. Model-predicted K' versus experimental K' for the ribose-5-phosphate isomerase and ribulose-phosphate 3-epimerase reactions. Open circles (GT-based K') are computed based on the Goldberg's database (25); filled squares (optimized K') are computed based on the optimized values of $\Delta_f G_i^0$ from Table 5.

Thus, the computed apparent equilibrium constants for these reactions do not depend on the experimental ionic composition. The validity of this assumption will be considered in the uncertainty and sensitivity analysis below. In addition, the predicted thermodynamic properties are not affected by the ionic strength for these reactions.

Optimal predicted $\Delta_f G_i^0$ associated with the $\Delta_r G^0$ predictions are listed in Table 5, compared to the optimal values of our previous version of the database (7). After the seven reactants of the pentose phosphate pathway and three constraints ($\Delta_r G^0$ of reaction PDH, AKGDH and SDH) are introduced, most of the estimated values of $\Delta_f G_i^0$ are shifted substantially. However, from Table 4 we can see that these shifts do not change the predicted $\Delta_r G^0$ compared to previous predictions. This is because the shifts in $\Delta_f G_i^0$ do not change the optimized results (apparent $\Delta_r G^0$ or K') of our model. Recall that here the estimated $\Delta_f G_i^0$ values represent parameters in a thermodynamic model for this set of interdependent biochemical reactions. Since the number of independent reactions for which data exist (29 reactions) is smaller than the number of $\Delta_f G_i^0$ values to represent the system (40 reactants), values for several reference species are set to either existing values or values reported elsewhere (Table 3). As a result, these $\Delta_f G_i^0$ values are not physical constants. Rather, they are parameters in a thermodynamic network model that together form a self-consistent picture of the thermodynamics of reactions of the set of reactants studied here.

The robustness of these calculations is checked by repeating the optimization with the $\Delta_f G_i^0$ for a single species constrained to a value $\pm 10\%$ different from the estimated optimal value. The degree to which the experimental data can be matched with one $\Delta_f G_i^0$ value 10% different

from the optimal values reported in Table 5 provides a measure of the sensitivity of the estimate. We define a sensitivity measure S_i for the estimate of $\Delta_f G_i^0$ as

$$E = \sum_{i=1}^M \left[\frac{1}{N_j} \sum_{j=1}^{N_j} \left(\Delta_r G_{\text{model}}^i - \Delta_r G_{\text{exp}}^{ij} \right)^2 \right], \quad (1)$$

$$S_i = \frac{\max(|E_i(\Delta_f G_i^0 \pm 0.1 \Delta_f G_i^0) - E_i(\Delta_f G_i^0)|)}{0.1 E_i(\Delta_f G_i^0)}, \quad (2)$$

where $E(\Delta_f G_i^0)$ is the optimal value of the error function (for values listed in Table 5) and $E(\Delta_f G_i^0 \pm 0.1 \Delta_f G_i^0)$ is the error with $\Delta_f G_i^0$ set to a 90% or 110% of its optimal value, M is the number of reactions, and N_j is the number of experimental measures for each reaction. Sensitivity values are listed in Table 5 for each species, revealing that estimates of $\Delta_f G_i^0$ for GLC^0 , $\text{NAD}_{\text{red}}^{2-}$, PYR^- , AKG^{2-} , SUC^{2-} , FUM^{2-} and COAS^0 are not highly sensitive to the data.

Predicted apparent Gibbs free energies under physiology conditions

The fifth column in Table 4 reports the predicted apparent $\Delta_r G^0$ ($= -RT \ln K'$) at physiological conditions representative of a muscle cell (26) ($T=310.15 \text{ K}$, $I=0.18 \text{ M}$, $\text{pH}=7$, $[\text{Mg}^{2+}]=0.8 \text{ mM}$, $[\text{K}^+]=140 \text{ mM}$, $[\text{Na}^+]=10 \text{ mM}$, $[\text{Ca}^{2+}]=0.0001 \text{ mM}$). Differences between the physiological free energies ($\Delta_r G^0$) and the standard free energies ($\Delta_r G_n^0$) are also shown in Table 4. These differences come from the effects of non-standard physiological conditions—temperature (T), ionic strength (I), pH and cation bindings. Therefore, the physiological free energy $\Delta_r G^0$ can be expressed by the summation of the standard free

Table 5. Optimal predicted $\Delta_f G_i^0$ for reference species ($T=298.15\text{ K}$, $I=0\text{ M}$)

No.	Species	$\Delta_f G_{i,n}^0$ ^a	$\Delta_f G_{i,o}^0$ ^a	$ \Delta_f G_{i,n}^0 - \Delta_f G_{i,o}^0 $	Sensitivity
1	GLC ⁰	-719.37	-916.39	197.02	0.33
2	ATP ⁴⁻	-2770.03	-2769.71	0.32	56099.52
3	F6P ²⁻	-1563.96	-1760.81	196.85	1.52
4	F16P ⁴⁻	-2401.08	-2597.60	196.52	3.55
5	DHAP ²⁻	-1194.65	-1292.91	98.26	3.51
6	GAP ²⁻	-1187.64	-1285.90	98.26	3.49
7	BPG ⁴⁻	-2276.28	-2354.55	78.27	19.44
8	NAD _{red} ²⁻	43.91	23.91	20.00	0.14
9	PG3 ³⁻	-1429.38	-1507.96	78.58	7.83
10	PG2 ³⁻	-1423.49	-1502.06	78.57	7.83
11	PEP ³⁻	-1190.84	-1269.40	78.56	5.54
12	PYR ⁻	-393.85	-472.72	78.87	0.64
13	OAA ²⁻	-714.06	-792.13	78.07	2.06
14	CIT ³⁻	-1022.44	-1157.52	135.08	1.38
15	ISCIT ³⁻	-1016.69	-1151.76	135.07	1.38
16	NADP _{ox} ³⁻	-834.79	-836.68	1.89	1837.57
17	AKG ²⁻	-676.45	-791.57	115.12	0.83
18	SUC ²⁻	-589.56	-685.56	96.00	0.91
19	GDP ³⁻	-1904.22	-1904.53	0.31	9560.62
20	FUM ²⁻	-500.99	-598.74	97.75	0.67
21	MAL ²⁻	-741.56	-839.30	97.74	1.44
22	G6P ²⁻	-1567.08	-1763.94 ^b	196.86	1.52
23	COA ⁵⁰	-57.17	0 ^b	57.17	0.03
24	NADP _{red} ⁴⁻	-787.35	-809.19 ^b	21.84	41.94
25	SUCCoA ⁻	-471.06	-509.59 ^b	38.53	3.47
26	E4P ²⁻	-1306.62	#	#	2.39
27	PGLT ²⁻	-1575.83	#	#	1.85
28	PGN ³⁻	-1782.55	#	#	2.34
29	R5P ²⁻	-1435.72	#	#	1.86
30	RUSP ²⁻	-1434.72	#	#	1.86
31	S7P ²⁻	-1685.66	#	#	1.31
32	X5P ²⁻	-1436.00	#	#	1.85

^a $\Delta_f G_{i,n}^0$ is the optimal free energies of formation in this work, $\Delta_f G_{i,o}^0$ is optimal free energies of formation in Li *et al.* (7). The unit of the free energy is kJ/mol.

^b $\Delta_f G_i^0$ of species is set as fixed value which is obtained from Alberty's database as in Li *et al.* (7).

energy $\Delta_r G^0$ and the non-standard contributions Δ_T , Δ_I , Δ_{pH} and Δ_P :

$$\Delta_r G^0(T, I) = -RT \ln K'(T, I) = \Delta_r G^0(T_0, I_0) + \Delta_T + \Delta_I + \Delta_{pH} + \Delta_P, \quad (3)$$

where $T_0=298.15\text{ K}$, $I_0=0\text{ M}$, K' is the apparent equilibrium constant for the associated biochemical reaction, Δ_T denotes the temperature contribution, Δ_I denotes the ionic strength contribution, Δ_{pH} denotes the pH contribution and Δ_P denotes the binding polynomial contribution.

An example calculation [for reaction GLK (EC 2.7.1.1)] is described in the Appendix A.

The contributions of non-standard elements to the differences between the standard free energy for the reference chemical reaction ($\Delta_r G^0$) and the physiological energy values ($\Delta_r G^0$) are listed in the last four columns of Table 4. The results can be divided to three cases: (i) if the stoichiometric coefficient of H^+ is non-zero in the reference chemical reaction ($\nu_H \neq 0$), the differences are substantial and pH contributes significantly, accounting for at least 73% of the difference, e.g. reactions GLK, PFK and GAP; (ii) if $\nu_H = 0$

($\Delta_{\text{pH}} = 0$) and $\sum v_i z_i^2 = 0$ ($\Delta_I = 0$), the differences tend to be relatively small compared with case (i) and temperature and/or binding polynomials contribute most to the differences, e.g. reactions PGI, TPI and ACON; (iii) if $v_{\text{H}} = 0$ ($\Delta_{\text{pH}} = 0$) and $\sum v_i z_i^2 \neq 0$, ionic strength and/or binding polynomials contribute most to the differences, e.g. reactions FBA, NPTH and PCL.

For the reactions of the pentose phosphate pathway, only the first three reactions G6PD, PGL and PGD show substantial difference between free energy for the reference chemical reaction ($\Delta_r G^0$) and for biochemical reaction ($\Delta_r G^0$) under physiological conditions. These three reactions have $v_{\text{H}} \neq 0$. They are the oxidative portion of the pentose phosphate pathway (15,23), which produce NADP_{red} and are essentially 'irreversible' *in vivo* (23).

Dissociation constants uncertainty and sensitivity analysis

The pK values listed in Table 2 are taken as the average value when there are several values (≥ 2) available in NIST database (27). For these pK values, the average value may not represent the best choice to be used in the model, i.e. some value among those available values may be more accurate than others. For some pK values, there exists only one estimate or no direct estimates. In order to predict the impact of uncertainty of these values on the model output, an uncertainty and sensitivity analysis is performed.

The following equation is used as a measure of uncertainty in a pK value when several independent measures are available:

$$U = u_i = \frac{pK_{i,\text{max}} - pK_{i,\text{min}}}{pK_i}, \quad (4)$$

where pK_{max} and pK_{min} refer to the maximum and minimum value of pK , respectively. Table 6 shows the computed uncertainties for these pK s.

Table 6. Dissociation constants uncertainty analysis for reactants with several pK values available in NIST database (27)

Reactant abbreviation	$U_{-pK_{\text{H1}}}$	$U_{-pK_{\text{H2}}}$	$U_{-pK_{\text{Mg1}}}$	$U_{-pK_{\text{Ca1}}}$
ADP	0.0539		0.0545	0.01748
ATP	0.0849		0.1051	0.1215
CIT	0.0423		0.0597	0.0480
GDP	0.0630			
GTP	0.0799		0.0835	
ISCIT	0.0052		0.0571	
MAL	0.0148	0.0153		0.0549
Pi	0.0251	0.0463	0.1975	0.1433
PEP	0.0336			
SUC	0.0133	0.0149	0.1476	
R5P	0.0016			

When only one pK value estimate is available, the uncertainty is defined as the average number \bar{u} of all calculated u_i :

$$U = \bar{u} = \frac{\sum_{i=1}^N u_i}{N}. \quad (5)$$

According to Table 6, \bar{u} is equal to 0.0609.

The sensitivities of the computed thermodynamic database due to a 10% change of pK values are calculated (28):

$$S_i = \frac{\partial E_i(x_i)/E_i(x_i)}{\partial x_i/x_i} \approx \frac{\max(|E_i(x_i \pm 0.1x_i) - E_i(x_i)|)}{0.1E_i(x_i)}, \quad (6)$$

where E is shown in equation (1), and x_i is the value of the i^{th} pK , Table 7 lists calculated sensitivities >0.1 . Sensitivity values for all potassium and sodium ion dissociation constants are <0.1 . Calcium ion dissociation constants are not included in these calculations because $[\text{Ca}^{2+}] = 0$ for all reactions in our raw-data database. Thus calculated sensitivities of calcium ion dissociations are equal to 0.

The product (US) combining uncertainty U and sensitivity S can be used to check the overlapping effect of uncertainty and sensitivity. For example, recall that we arbitrarily assign the value of 4.995 to the pK_{H1} for PGN. Since the value is not available in NIST database, its uncertainty U is set to the average number 0.0609. If we consider the theoretical range of 4–5.99 discussed above, then the

Table 7. Sensitivity >0.1 in dissociation constants sensitivity analysis

Reactant abbreviation	$S_{-pK_{\text{H1}}}$	$S_{-pK_{\text{H2}}}$	$S_{-pK_{\text{Mg1}}}$	$S_{-pK_{\text{Mg2}}}$
ADP	0.4936		0.3696	0.1709
ATP	0.2151		0.2665	0.2210
CIT			0.6029	
COAS	0.5344			
DHAP	0.6591		0.3772	
F16P	1.1839	0.3181	1.3545	
G6P	0.6372		0.4524	
GDP			0.1873	
GTP			0.1310	
ISCIT	0.1230		0.2245	
NADP_{ox}	1.7916			
NADP_{red}	0.7611			
Pi	0.1248		0.2015	
PG2	1.2172			
PG3	0.3698			
PEP	0.2293			
R5P	0.1818			
RU5P	0.1007			
S7P	0.1433			
X5P	0.1597			

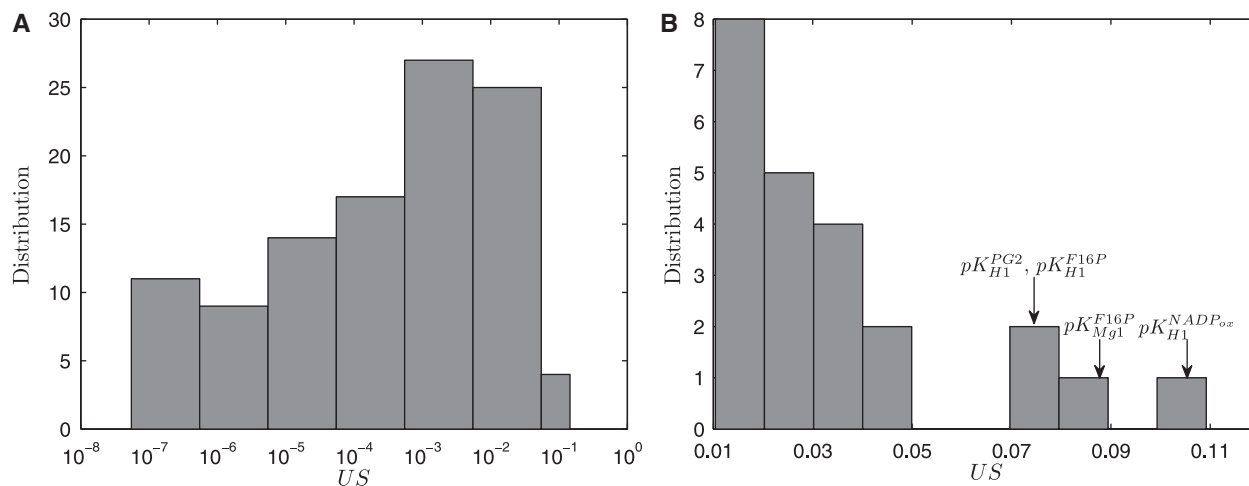


Figure 3. (A) Distribution of the product of uncertainty and sensitivity (US) for all pK values; (B) detailed distribution of the product >0.01 .

calculated uncertainty U is ~ 0.4 . For this case, because the computed pK_{H1} sensitivity is 0.0225, the US product is <0.01 , which is small enough that the value of pK_{H1} for PGN has no substantial effect on the model output. Similarly, recall that E4P, RU5P, S7P and X5P are assumed to have dissociation properties equivalent to R5P in our calculations. Although the computed pK sensitivities of E4P, RU5P, S7P and X5P are $3.81E-6$, 0.1007, 0.1433 and 0.1597, respectively, all the US products of the pK_{H1} for these reactants are <0.01 . Therefore, the assumption of equivalent dissociation properties for E4P, R5P, RU5P, S7P and X5P does not substantially effect our calculations.

Figure 3A illustrates that US products span eight orders of magnitude. Figure 3B illustrates the detailed distribution of the US products >0.01 . All US products are <0.11 . There are 23 cases for which $US > 0.01$. These 23 US values belong to 15 reactants and four pK s as listed in Table 8. They are a subset of the pK s with sensitivity >0.1 . They demonstrate the most important pK s which can make obvious impact on the model output. The largest four US values are $pK_{H1}^{NADP_{ox}}$, pK_{Mg1}^{F16P} , pK_{H1}^{PG2} and pK_{H1}^{F16P} , as indicated in Figure 3B.

Database dissemination

ThermoML is an extensible markup language (XML)-based approach, which is an IUPAC standard for storage and exchange of thermodynamic property data (29–32). Our optimized results are stored in the standard ThermoML format with two small extensions to the current ThermoML schema (32): (i) adding ‘pseudo-Gibbs free energy of formation, kJ/mol’ in the list of $ePropName$ in *BioProperties* of *PureOrMixtureData*; and (ii) adding ‘biochemical network calculation’ in $ePredictionType$ of *Prediction*. We use the term ‘pseudo-Gibbs free energy of formation’ because in

Table 8. The product (US) >0.01 in dissociation constants uncertainty and sensitivity analysis

Reactant abbreviation	pK s
ADP	$pK_{H1}, pK_{Mg1}, pK_{Mg2}$
ATP	$pK_{H1}, pK_{Mg1}, pK_{Mg2}$
CIT	pK_{Mg1}
COAS	pK_{H1}
DHAP	pK_{H1}, pK_{Mg1}
F16P	$pK_{H1}, pK_{H2}, pK_{Mg1}$
G6P	pK_{H1}, pK_{Mg1}
GDP	pK_{Mg1}
GTP	pK_{Mg1}
ISCIT	pK_{Mg1}
Pi	pK_{Mg1}
NADP _{ox}	pK_{H1}
NADP _{red}	pK_{H1}
PG2	pK_{H1}
PG3	pK_{H1}

our thermodynamic model the estimated $\Delta_r G_i^0$ values represent adjustable parameters for the given set of interdependent biochemical reactions. In our ThermoML data files, the abbreviation name of reactant is also added in $sCommonName$ in *Compound*. In the ThermoML reaction database, if the value of $\Delta_r H_i^0$ is not available, it is specified in $sPredictionMethodDescription$, and both $nPropValue$ and $nPropDigits$ are set to 0 in *PropertyValue* of *NumValues*. The ThermoML schema and our ThermoML data files are provided in [Supplementary Data](#).

Discussion

We have updated our biochemical thermodynamic database by adding the reactions of the pentose phosphate pathway. To build the new database, each original publication has been studied on a case-by-case basis, case-specific assumptions and approximations determined and documented, and case-specific calculations performed and documented. Raw data and documented estimations of solution properties are made electronically available so that the updated database remains transparent and extensible.

The developed database is optimally self-consistent and consistent with the data available for reactions considered and the constraints. Theoretical predictions of apparent equilibrium constants optimally match experimental data on equilibrium constants. These apparent equilibrium constants are predicted based on the estimated species-level Gibbs free energies of formation and accounting for the effects of temperature, ionic interactions and hydrogen and metal cation binding. The new database provides thermodynamic and network-based estimates of thermodynamic properties for six reactions of the pentose phosphate pathway for which estimates are not available in the pre-existing literature.

These calculations demonstrate how network thermodynamic calculations are effectively extended. Adding raw experimental data on reactions and reactants of the pentose phosphate pathway into corresponding raw-data database, reaction database and reactant database, respectively, a previous thermodynamic network model was extended to include these elements.

Although the new optimal estimates of $\Delta_r G^0$ for reactants of glycolysis and tricarboxylic acid cycle are equal to previous estimates (7), most of the optimal predicted $\Delta_r G_i^0$ values which are associated with the $\Delta_r G^0$ predictions are shifted compared to the previous version. This result demonstrates that reliable and self-consistent extensions require the recalculation of entire set of species-level parameters. Furthermore, sensitivity analysis reveals that some formation energies can vary substantially without changing the optimized objective value significantly. While this set of optimal values represents a self-consistent set, combining these estimated formation energies with independently estimated parameters from other studies would require re-optimizing a combined database.

The uncertainty and sensitivity analysis of dissociation constants reveals 23 pK_s most important to the model output. Additional experimental measurements of these parameter values are desirable.

Supplementary Data

Supplementary data are available at Database Online.

Acknowledgements

The authors are grateful to Robert Goldberg for advice and critical comments.

Funding

National Institutes of Health Heart Lung and Blood Institute (grant number HL072011). Funding for open access charge: National Institutes of Health Heart Lung and Blood Institute.

Conflict of interest. None declared.

References

1. Vojinović, V. and von Stockar, U. (2009) Influence of uncertainties in pH, pMg, activity coefficients, metabolite concentrations, and other factors on the analysis of the thermodynamic feasibility of metabolic pathways. *Biotechnol. Bioeng.*, **103**, 780–795.
2. Mavrovouniotis, M.L. (1993) Identification of localized and distributed bottlenecks in metabolic pathways. In: Hunter, L., Searls, D.B. and Shavlik, J.W. (eds), *Proceedings of the First International Conference on Intelligent Systems for Molecular Biology*. AAAI Press, Bethesda, MD, pp. 275–283.
3. Yang, F. and Beard, D.A. (2006) Thermodynamically based profiling of drug metabolism and drug-drug metabolic interactions: a case study of acetaminophen and ethanol toxic interaction. *Biophys. Chem.*, **120**, 121–134.
4. Kümmel, A., Panke, S. and Heinemann, M. (2006) Putative regulatory sites unraveled by network-embedded thermodynamic analysis of metabolome data. *Mol. Syst. Biol.*, **2**, 2006.0034.
5. Henry, C.S., Broadbelt, L.J. and Hatzimanikatis, V. (2007) Thermodynamics-based metabolic flux analysis. *Biophys. J.*, **92**, 1792–1805.
6. Vinnakota, K.C., Wu, F., Kushmerick, M.J. et al. (2009) Multiple ion binding equilibria, reaction kinetics, and thermodynamics in dynamic models of biochemical pathways. *Methods Enzymol.*, **454**, 29–68.
7. Li, X., Dash, R.K., Pradhan, R.K. et al. (2010) A database of thermodynamic quantities for the reactions of glycolysis and the tricarboxylic acid cycle. *J. Phys. Chem.*, **114**, 16068–16082.
8. Alberty, R.A. (2003) *Thermodynamics of Biochemical Reactions*. John Wiley, Hoboken, NJ.
9. Beard, D.A. and Qian, H. (2008) Conventions and calculations for biochemical systems. In: *Chemical Biophysics: Quantitative Analysis of Cellular Systems*. Cambridge University Press, Cambridge, UK, pp. 24–40.
10. Alberty, R.A. (2006) Thermodynamic properties of weak acids involved in enzyme-catalyzed reactions. *J. Phys. Chem. B*, **110**, 5012–5016.
11. Clarke, E.C.W. and Glew, D.N. (1980) Evaluation of Debye–Hückel limiting slopes for water between 0 and 150°C. *J. Chem. Soc., Faraday Trans. 1*, **76**, 1911–1916.
12. Alberty, R.A. (2001) Effect of temperature on standard transformed Gibbs energies of formation of reactants at specified pH and ionic strength and apparent equilibrium constants of biochemical reactions. *J. Phys. Chem. B*, **105**, 7865–7870.
13. Alberty, R.A. (2005) Calculation of thermodynamic properties of species of biochemical reactants using the inverse legendre transform. *J. Phys. Chem. B*, **109**, 9132–9139.

14. Glaser, L. and Brown, D.H. (1955) Purification and properties of D-glucose-6-phosphate dehydrogenase. *J. Biol. Chem.*, **216**, 67–79.
15. Casazza, J.P. and Veech, R.L. (1986) The interdependence of glycolytic and pentose cycle intermediates in ad libitum fed rats. *J. Biol. Chem.*, **261**, 690–698.
16. Villet, R.H. and Dalziel, K. (1969) The nature of the carbon dioxide substrate and equilibrium constant of the 6-phosphogluconate dehydrogenase reaction. *Biochem. J.*, **115**, 633–638.
17. Axelrod, B. and Jang, R. (1954) Purification and Properties of Phosphoriboisomerase from Alfalfa. *J. Biol. Chem.*, **209**, 847–855.
18. Hurwitz, J. and Horecker, B.L. (1956) The purification of phosphoketopentose epimerase from lactobacillus pentosus and the preparation of xylulose 5-phosphate. *J. Biol. Chem.*, **223**, 993–1008.
19. Datta, A.G. and Racker, E. (1961) Mechanism of action of transketolase. *J. Biol. Chem.*, **236**, 617–623.
20. Goldberg, R.N., Tewari, Y.B., Bell, D. et al. (1993) Thermodynamics of enzyme-catalyzed reactions: Part 1. Oxidoreductases. *J. Phys. Chem. Ref. Data*, **22**, 515–82.
21. Goldberg, R.N. and Tewari, Y.B. (1994) Thermodynamics of enzyme-catalyzed reactions: Part 2. Transferases. *J. Phys. Chem. Ref. Data*, **23**, 547–617.
22. Goldberg, R.N. and Tewari, Y.B. (1995) Thermodynamics of enzyme-catalyzed reactions: Part 5. Isomerases and ligases. *J. Phys. Chem. Ref. Data*, **24**, 1765–1801.
23. Nelson, D.L. and Cox, M.M. (2005) Glycolysis, gluconeogenesis, and the pentose phosphate pathway. In: *Lehninger Principle of Biochemistry*. W. H. Freeman and Company Press, New York.
24. Perrin, D.D., Dempsey, B. and Serjeant, E.P. (1981) *pKa Prediction for Organic Acids and Bases*. Chapman and Hall, London and New York.
25. Goldberg, R.N. and Tewari, Y.B. (1989) Thermodynamic and transport properties of carbohydrates and their monophosphates: the pentoses and hexoses. *J. Phys. Chem. Ref. Data*, **18**, 809–880.
26. Godt, R.E. and Maughan, D.W. (1988) On the composition of the cytosol of relaxed skeletal muscle of the frog. *Am. J. Physiol. Cell Physiol.*, **254**, C591–C604.
27. Smith, R.M., Martell, A.E. and Motekaitis, R.J. (2004) NIST standard reference database 46 version 8.0: NIST critically selected stability constants of metal complexes. In: *NIST Standard Reference Data*. Gaithersburg, MD.
28. Wu, F., Yang, F., Vinnakota, K.C. et al. (2007) Computer modeling of mitochondrial tricarboxylic acid cycle, oxidative phosphorylation, metabolite transport, and electrophysiology. *J. Biol. Chem.*, **282**, 24525–24537.
29. Frenkel, M., Chirico, R.D., Diky, V.V. et al. (2002) ThermoML - an XML-based approach for storage and exchange of experimental and critically evaluated thermophysical and thermochemical property data. 1. Experimental data. *J. Chem. Eng. Data*, **48**, 2–13.
30. Chirico, R.D., Frenkel, M., Diky, V.V. et al. (2003) ThermoML - an XML-based approach for storage and exchange of experimental and critically evaluated thermophysical and thermochemical property data. 2. Uncertainties. *J. Chem. Eng. Data*, **48**, 1344–1359.
31. Frenkel, M., Chirico, R.D., Diky, V.V. et al. (2004) ThermoML - an XML-based approach for storage and exchange of experimental and critically evaluated thermophysical and thermochemical property data. 3. Critically evaluated data, predicted data, and equation representation. *J. Chem. Eng. Data*, **49**, 381–393.
32. Chirico, R.D., Frenkel, M., Diky, V. et al. (2009) ThermoML - an XML-based approach for storage and exchange of experimental and critically evaluated thermophysical and thermochemical property data. 4. Biomaterials. *J. Chem. Eng. Data*, **55**, 1564–1572.
33. Goldberg, R.N. and Tewari, Y.B. (1994) Thermodynamics of enzyme-catalyzed reactions. Part 3. Hydrolases. *J. Phys. Chem. Ref. Data*, **23**, 1035–1103.
34. Alberty, R.A. (1995) Standard transformed formation properties of carbon dioxide in aqueous solutions at specified pH. *J. Phys. Chem.*, **99**, 11028–11034.
35. Tewari, Y.B., Steckler, D.K., Goldberg, R.N. et al. (1988) Thermodynamics of hydrolysis of sugar phosphates. *J. Biol. Chem.*, **263**, 3670–3675.
36. Martell, A.E., Smith, R.M. and Motekaitis, R.J. (2004) NIST standard reference database 46 version 8.0: NIST critically selected stability constants of metal complexes. In: *NIST Standard Reference Data*. Gaithersburg, MD.
37. Larsson-Raźnikiewicz, M. (1972) Complex formation between 3-phospho-D-glyceric acid and divalent metal ions. *European Journal of Biochemistry*, **30**, 579–583.
38. Merrill, D.K., McAlexander, J.C. and Guynn, R.W. (1981) Equilibrium constants under physiological conditions for the reactions of -3-phosphoglycerate dehydrogenase and -phosphoserine aminotransferase. *Arch. Biochem. Biophys.*, **212**, 717–729.
39. Briggs, T.N. and Stuehr, J.E. (1975) Simultaneous potentiometric determination of precise equivalence points and pK values of two- and three-pK systems. *Anal. Chem.*, **47**, 1916–1920.

Appendix A

Calculating the physiological free energy $\Delta_r G^0$

The standard free energy $\Delta_r G^0$ can be calculated based on the equilibrium constant K , for a reference chemical reaction:

$$\Delta_r G^0(T_0, I_0) = -RT_0 \ln K(T_0, I_0), \quad (\text{A.1})$$

where $T_0 = 298.15 \text{ K}$, $I_0 = 0 \text{ M}$, $R = 8.3145 \text{ J K}^{-1} \text{ mol}^{-1}$.

The apparent equilibrium constant, K' , for the associated biochemical reaction can also be calculated based on K :

$$K' = K[\text{H}^+]^{-\nu_H} \prod_{j=1}^N P_j^{\nu_j}, \quad (\text{A.2})$$

where ν_H is the stoichiometric coefficient associated with H^+ in the reference reaction, P_j is the binding polynomial associated with species j and ν_j is the stoichiometric coefficient of species j . If assuming that the activity coefficient for hydrogen ion is equal to 1, i.e. $\text{pH} = -\log_{10}([\text{H}^+])$, the physiological free energy $\Delta_r G^0$ can then be obtained based on equations (A.1) and (A.2):

$$\Delta_r G^0(T, I) = -RT \ln K'(T, I) = -RT \ln K(T, I) - 2.303RT \times \nu_H \times \text{pH} - RT \ln \left(\prod_{j=1}^N P_j^{\nu_j} \right). \quad (\text{A.3})$$

The first term in the right-hand side of equation (A.3) can be separated into four terms as shown in equation (A.6) based on equations (A.4) and (A.5) (7):

$$\begin{aligned} pK(T,I) = & pK(T_0,I_0) + \frac{\Delta_r H^0(I_0)}{2.303R} \left(\frac{1}{T} - \frac{1}{T_0} \right) \\ & + \frac{\alpha(T)}{2.303} \left(\frac{I_0^{1/2}}{1 + BI_0^{1/2}} - \frac{I^{1/2}}{1 + BI^{1/2}} \right) \sum v_i z_i^2, \end{aligned} \quad (\text{A.4})$$

$$\alpha(T) = 1.10708 - (1.54508 \times 10^{-3})T + (5.95584 \times 10^{-6})T^2, \quad (\text{A.5})$$

$$\begin{aligned} -RT \ln K(T,I) = & -RT \ln K(T_0,I_0) + \Delta_r H^0(I_0) \left(1 - \frac{T}{T_0} \right) + \\ & RT \alpha(T) \left(\frac{I_0^{1/2}}{1 + BI_0^{1/2}} - \frac{I^{1/2}}{1 + BI^{1/2}} \right) \sum v_i z_i^2 \\ = & -RT_0 \ln K(T_0,I_0) + RT \ln K(T_0,I_0) \left(\frac{T_0}{T} - 1 \right) + \Delta_r H^0(I_0) \left(1 - \frac{T}{T_0} \right) \\ & + RT \alpha(T) \left(\frac{I_0^{1/2}}{1 + BI_0^{1/2}} - \frac{I^{1/2}}{1 + BI^{1/2}} \right) \sum v_i z_i^2 \end{aligned} \quad (\text{A.6})$$

where pK is the negative base-10 logarithm of equilibrium constant K , $\Delta_r H^0(I_0)$ is the standard reaction enthalpy at ionic strength I_0 , z_i is the valence of species i , B is an empirical constant taken to be $1.6 \text{ M}^{-1/2}$, and $\alpha(T)$ is the coefficient in the Debye equation $\ln \gamma = -\alpha z^2 I^{1/2}$.

The non-standard element (temperature, ionic strength, pH and binding polynomial) contributions Δ_T , Δ_I , Δ_{pH} and Δ_p are defined as follows:

$$\Delta_T = RT \ln K(T_0,I_0) \left(\frac{T_0}{T} - 1 \right) + \Delta_r H^0(I_0) \left(1 - \frac{T}{T_0} \right), \quad (\text{A.7})$$

$$\Delta_I = RT \alpha(T) \left(\frac{I_0^{1/2}}{1 + BI_0^{1/2}} - \frac{I^{1/2}}{1 + BI^{1/2}} \right) \sum v_i z_i^2, \quad (\text{A.8})$$

$$\Delta_{pH} = -2.303RT \times v_H \times \text{pH}, \quad (\text{A.9})$$

$$\Delta_p = -RT \ln \left(\prod_{j=1}^N P_j^{v_j} \right). \quad (\text{A.10})$$

Then the physiological free energy $\Delta_r G^0$ can be expressed by the summation of the standard free energy $\Delta_r G^0$ and the non-standard element contributions Δ_T , Δ_I , Δ_{pH} and Δ_p :

$$\Delta_r G^0(T,I) = \Delta_r G^0(T_0,I_0) + \Delta_T + \Delta_I + \Delta_{pH} + \Delta_p. \quad (\text{A.11})$$

Example

The calculations the physiological free energy $\Delta_r G^0$ for reaction glucokinase GLK (EC 2.7.1.1) is illustrated as an example. As mentioned in the article, the physiological conditions are $T=310.15 \text{ K}$, $I=0.18 \text{ M}$, $\text{pH}=7$,

$[\text{Mg}^{2+}] = 0.8 \text{ mM}$, $[\text{K}^+] = 140 \text{ mM}$, $[\text{Na}^+] = 10 \text{ mM}$, $[\text{Ca}^{2+}] = 0.0001 \text{ mM}$. The optimized standard free energy ($\Delta_r G^0$) of GLK is 16.19 kJ/mol , as shown in Table 4. Equilibrium constant for the chemical reference reaction can be computed as $K = \exp(-\Delta_r G^0/RT) = 1.46 \times 10^{-3}$. The chemical reference reaction of GLK is



$v_H = 1$ in this reference reaction, and $\sum v_i z_i^2 = 1 \times (-2)^2 + 1 \times (-3)^2 + 1 \times 1^2 - 1 \times 0^2 - 1 \times (-4)^2 = -2$. Thus, the pH and ionic strength contributions can be calculated as follows:

$$\begin{aligned} \Delta_{pH} = & -2.303RT \times v_H \times \text{pH} = -2.303 \times (8.3145 \times 10^{-3}) \\ & \times 310.15 \times 1 \times 7 = -41.56 \text{ (kJ/mol)} \end{aligned}$$

$$\begin{aligned} \alpha(T) = & 1.10708 - (1.54508 \times 10^{-3}) \times 310.15 \\ & + (5.95584 \times 10^{-6}) \times 310.15^2 = 1.2008, \end{aligned}$$

$$\begin{aligned} \Delta_I = & RT \alpha(T) \left(\frac{I_0^{1/2}}{1 + BI_0^{1/2}} - \frac{I^{1/2}}{1 + BI^{1/2}} \right) \sum v_i z_i^2 \\ = & (8.3145 \times 10^{-3}) \times 310.15 \times 1.2008 \\ & \times \left(0 - \frac{0.18^{1/2}}{1 + 1.6 \times 0.18^{1/2}} \right) \times (-2) = 1.57 \text{ (kJ/mol)}. \end{aligned}$$

As shown in Table 1 in the article, $\Delta_r H^0(I=0) = -23.8 \text{ kJ/mol}$. Then temperature contribution can be obtained

$$\begin{aligned} \Delta_T = & RT \ln K(T_0,I_0) \left(\frac{T_0}{T} - 1 \right) + \Delta_r H^0(I_0) \left(1 - \frac{T}{T_0} \right) \\ = & (8.3145 \times 10^{-3}) \times 310.15 \times \ln(1.46 \times 10^{-3}) \\ & \times \left(\frac{298.15}{310.15} - 1 \right) + (-23.8) \times \left(1 - \frac{310.15}{298.15} \right) \\ = & 1.61 \text{ (kJ/mol)}. \end{aligned}$$

In order to calculate binding polynomial contribution Δ_p , the binding polynomial P_j for each reactant j should be first calculated (7):

$$\begin{aligned} P_j = & 1 + \frac{10^{-\text{pH}}}{K_{H1}} + \frac{10^{-2\text{pH}}}{K_{H1}K_{H2}} + \frac{[\text{Mg}^{2+}]}{K_{Mg1}} + \frac{10^{-\text{pH}}[\text{Mg}^{2+}]}{K_{H1}K_{HMg}} \\ & + \frac{[\text{Mg}^{2+}]^2}{K_{Mg1}K_{Mg2}} + \dots \end{aligned} \quad (\text{A.12})$$

where K_{di} is the dissociation constant of cation ion d . The negative base-10 logarithm of dissociation constant pK_{di} ($pK_{di} = -\log K_{di}$) for all reactants are listed in Table 2 in the article. Temperature and ionic strength should be done to transform all the dissociation constants to $T=310.15 \text{ K}$ and $I=0.18 \text{ M}$ before calculating the binding polynomial P_j . For reaction GLK,

$$\begin{aligned} \Delta_p = & -RT \ln \left(\frac{P_{G6P} \times P_{ADP}}{P_{GLC} \times P_{ATP}} \right) = -(8.3145 \times 10^{-3}) \times 310.15 \\ & \times \ln \left(\frac{1.0978 \times 3.4834}{1 \times 12.1245} \right) = 2.97 \text{ (kJ/mol)}. \end{aligned}$$

Therefore, the physiological free energy for reaction glucokinase GLK is

$$\begin{aligned}\Delta_r G^0 &= \Delta_r G^0 + \Delta_T + \Delta_I + \Delta_{\text{pH}} + \Delta_P \\ &= 16.19 + 1.61 + 1.57 - 41.56 + 2.97 \\ &= -19.22 \text{ (kJ/mol)}.\end{aligned}$$

The total difference is $\Delta_{\text{tot}} = \Delta_T + \Delta_I + \Delta_{\text{pH}} + \Delta_P = 1.61 + 1.57 - 41.56 + 2.97 = -35.41$ (kJ/mol). The percentages of the contributions of non-standard elements to this difference are

$$T\% = \frac{\Delta_T}{\Delta_{\text{tot}}} \times 100\% = -5\%,$$

$$I\% = \frac{\Delta_I}{\Delta_{\text{tot}}} \times 100\% = -4\%,$$

$$\text{pH}\% = \frac{\Delta_{\text{pH}}}{\Delta_{\text{tot}}} \times 100\% = 117\%,$$

$$P\% = \frac{\Delta_P}{\Delta_{\text{tot}}} \times 100\% = -8\%.$$

Nomenclature

B: an empirical constant taken to be $1.6 \text{ M}^{-1/2}$

E: the minimum squared difference between model simulations and experimental data

$\Delta_r G^0$: standard Gibbs free energy of reaction

$\Delta_f G_i^0$: standard Gibbs free energy of formation of species *i*

$\Delta_r G^0$: apparent Gibbs free energy of reaction

$\Delta_d H_{K_d}$: enthalpy of proton/metal cation dissociation

$\Delta_r H^0$: standard enthalpy of reaction

I: ionic strength

K: chemical (reference reaction) equilibrium constant

K': apparent equilibrium constant

$K_{d,i}$: the dissociation constant of cation ion *d*

M: the number of reactions

N: the number of *pK*s which have several values available in NIST database

N_j : the number of experimental data in each reaction

P_j : binding polynomial associated with reactant *j*

pK: negative logarithm of the dissociation constant

R: gas constant, $8.3145 \text{ J K}^{-1} \text{ mol}^{-1}$

S: sensitivity

T: temperature

U: uncertainty

v_i : stoichiometric coefficient for species *i* in a given reaction

z_i : valence of species *i*

Δ_I : the ionic strength contribution

Δ_{pH} : the pH contribution

Δ_P : the binding polynomial contribution

Δ_T : the temperature contribution